Biomaterials 32 (2011) 1635–1645

Contents lists available at ScienceDirect

Biomaterials

journal homepage: www.elsevier.com/locate/biomaterials

# Curcumin-decorated nanoliposomes with very high affinity for amyloid-β1-42 peptide

Spyridon Mourtas [a], Mara Canovi [b], Cristiano Zona [c], Dario Aurilia [c], Anna Niarakis [a], Barbara La Ferla [c], Mario Salmona [b], Francesco Nicotra [c], Marco Gobbi [b], Sophia G. Antimisiaris [a,d,*]

[a] Laboratory of Pharmaceutical Technology, Department of Pharmacy, University of Patras, Rio 26510, Patras, Greece
[b] Department of Biochemistry and Molecular Pharmacology, Istituto di Ricerche Farmacologiche "Mario Negri", 20156 Milano, Italy
[c] Department of Biotechnology and Bioscience, University of Milano-Bicocca, 20126 Milano, Italy
[d] Institute of Chemical Engineering and High Temperatures, FORTH/ICE-HT, Rio 26504, Patras, Greece

ARTICLE INFO

*Article history:*
Received 13 October 2010
Accepted 13 October 2010
Available online 4 December 2010

*Keywords:*
Alzheimer disease (AD)
Amyloid beta (Aβ)
Curcumin
Click chemistry
Structure
Liposomes

ABSTRACT

Amyloid β (Aβ) aggregates are considered as possible targets for therapy and/or diagnosis of Alzheimer disease (AD). It has been previously shown that curcumin targets Aβ plaques and interferes with their formation, suggesting a potential role for prevention or treatment of AD. Herein, a click chemistry method was used to generate nanoliposomes decorated with a curcumin derivative, designed to maintain the planar structure required for interaction with Aβ, as directly confirmed by Surface Plasmon Resonance experiments. Another type of liposomes was formed starting from curcumin-phospholipid conjugate, in which the planar structure of curcumin is disrupted. Both types of generated curcumin-decorated vesicles had mean diameters in the nano range (131–207 nm) and slightly negative ζ-potential values according to their lipid composition, and were stable for periods up to 20 days. They also demonstrated high integrity during incubation in presence of plasma proteins. Surface Plasmon Resonance experiments, measuring the binding of flowing liposomes to immobilized Aβ1-42, indicated that the liposomes exposing the curcumin derivative (maintaining the planarity) have extremely high affinity for Aβ1-42 fibrils (1–5 nM), likely because of the occurrence of multivalent interactions, whereas those exposing non-planar curcumin did not bind to Aβ1-42. In summary, we describe here the preparation and characterization of new nanoparticles with a very high affinity for Aβ1-42 fibrils, to be exploited as vectors for the targeted delivery of new diagnostic and therapeutic molecules for AD.



## 1. Introduction

Alzheimer's disease (AD) is the most common form of dementia among neurodegenerative diseases in the elderly population, and the fourth common cause of death in Western countries after heart disease, cancer and stroke [1–3]. More than 5 million Americans and 3 million Europeans are believed to have AD, while these numbers are estimated to increase to 15 million [1–3] and more than 6 million in the next 40 years, respectively [4,5], due to increase of the elderly population.

The mechanisms underlying AD are not yet completely clear, and there is still no cure. However, in recent years, several approaches aimed at inhibiting disease progression have advanced to clinical trials. Among these, strategies targeting the production and clearance of the amyloid-beta (Aβ) peptide are the most advanced [6]. Indeed, genetic, pathological and biochemical clues suggest that the progressive production and subsequent accumulation of Aβ, plays a central role in AD pathogenesis [7,8]. The predominant and initial peptide deposited in the brain parenchyma is Aβ1-42 [9], a highly fibrillogenic [10] peptide which is believed to follow metal induced aggregation to form plaques [11]. Oligomers appearing before plaque deposition in an early stage of AD pathology have been indicated as the most toxic Aβ species [12–18]. Targeting Aβ1-42 in all its aggregation forms has been suggested for therapeutic and/or diagnostic purposes [17–22]. Moreover, it has been recently demonstrated that brain and blood Aβ are in equilibrium through the blood brain barrier (BBB), and sequestration of Aβ in the blood may shift this equilibrium, drawing out the excess from the brain ("sink" effect) [23,24]. According to this finding, blood circulating Aβ peptides could also be potential targets for the therapy of AD.

Curcumin is a naturally occurring phytochemical. It has been shown to be a potent anti-oxidant and anti-inflammatory compound with a favorable toxicity profile [25]; and a free (nitric oxide–based)

* Corresponding author. Laboratory of Pharmaceutical Technology, Department of Pharmacy, University of Patras, Rio 26510, Patras, Greece. Tel.: +30 2610 969332; fax: +30 2610996302.
*E-mail address:* santimis@upatras.gr (S.G. Antimisiaris).

0142-9612/$ – see front matter © 2010 Elsevier Ltd. All rights reserved.
doi:10.1016/j.biomaterials.2010.10.027

radical scavenger [26], which protects the brain from lipid peroxidation [27]. Curcumin inhibits amyloid Aβ1-42 oligomer formation and cell toxicity at micromolar concentrations *in vitro*, [28–32] and binds to plaques reducing amyloid levels in vivo [30]. Thus, it has been hypothesized that its extensive use might account for the significantly lower prevalence of AD in the Asian–Indian population [33] and that curcumin treatment might be beneficial for AD patients. The ability of curcumin to bind Aβ peptides and inhibit its aggregation has been attributed to three structural features of the curcumin molecule: the presence of two aromatic end groups and their co-planarity, the substitution pattern of these aromatics, and the length (8–16 Å) and rigidity of the linker region [34].

Current strategies include development of curcumin analogues with similar biological activity but improved pharmacokinetics, bioavailability, water solubility and stability at physiological conditions [35–38]. Another possibility for the application of the beneficial effects of curcumin could be the attachment of curcumin, in a stable way and active structural conformation, on the surface of biocompatible/biodegradable and stealth nanoparticles. Such attachment (on the surface of nanoparticles), might help increase the drug bioavailability and perhaps it will further increase the binding affinity of curcumin for Aβ peptides, due to multivalency [39–41], as well. Among the known nanoparticle types, liposomes have many advantages for drug delivery applications due to their non-toxic and non-immunogenic, fully biodegradable and structurally versatile nature [42].

In the present study we designed and formulated two types of nanosized liposomes functionalized with curcumin derivatives (on their surface) and evaluated their ability to bind to Aβ fibrils by Surface Plasmon Resonance. The two types of decorated liposomes were obtained either by a conventional synthetic method or a click chemistry technique [43–46]. When the conventional synthetic method is used (conjugation of curcumin with functionalized phospholipid and use of this lipid conjugate for liposome formation), the planarity of the curcumin molecule is disrupted due to the introduction of a tetra-substituted carbon atom in the linker region. On the contrary, the click chemistry technique allowed conjugation of an appropriate curcumin derivative, designed in order to preserve the planarity of the compound and opportunely functionalized for the conjugation.

## 2. Materials and methods

### 2.1. Materials

#### 2.1.1. For lipid conjugate synthesis

All commercial chemicals were purchased from Sigma–Aldrich except O-(2-azidoethyl)-O′-(N-diglycolyl—2-aminoethyl)heptaethyleneglycol which was purchased from Novabiochem and 1,2-Dipalmitoyl-*sn*-Glycero-3-Phosphothioethanol (Sodium Salt) which was obtained from Avanti polar lipids. All chemicals were used without further purification, while all required anhydrous solvents were dried with molecular sieves, for at least 24 h prior to use. Thin layer chromatography (TLC) was performed on silica gel 60 F254 plates (Merck) with detection using UV light when possible, or by charring with a solution of $(NH_4)_6Mo_7O_{24}$ (21 g), $Ce(SO_4)_2$ (1 g), concentrated $H_2SO_4$ (31 mL) in water (500 mL) or with an ethanol solution of ninhydrin or with Dragendorff' spray reagent [47] or molybdenum blue spray [48]. Flash column chromatography was performed on silica gel 230–400 mesh (Merck). $^1H$ and $^{13}C$ NMR spectra were recorded at 25 °C unless otherwise stated, with a Varian Mercury 400 MHz instrument. Chemical shift assignments, reported in ppm, are referenced to the corresponding solvent peaks. MS were recorded either on a QTRAP system with ESI source (Applied Biosystem) while HRMS were registered on a QSTAR elite system with a nanospray ion source (Applied Biosystem).

#### 2.1.2. For nanoliposome preparation

Phosphaditidyl choline (PC), 1,2-distearoyl-sn-glycerol-3-phosphatidylcholine (DSPC), 1,2-dipalmitoyl-sn-glycerol-3-phosphatidylcholine (DPPC), 1,2-dipalmitoyl-sn-glycerol-3-phosphatidyl glycerol (DPPG), were purchased from Avanti Polar Lipids. Cholesterol (Chol), Sephadex G50 (course,) 5,6 carboxyflouorescein (CF), calcein, Sepharose CL-4B were purchased from Sigma–Aldrich. Spectrapore Dialysis tubing (MW cutoff 10000) was from Serva.

All other chemicals were reagent grade. Ultrapure water was produced with a Millipore Direct-Q system.

### 2.2. Synthesis of lipid and curcumin derivatives for click chemistry

For the preparation of curcumin-decorated liposomes by the click reaction, two specific compounds were synthesized; a lipid-peg-azide compound (3-deoxy-1,2-dipalmitoyl-3-(4′-methyl (O-(2-azidoethyl)-heptaethylenglycol-2-yl)-ethylcarbamoylmethoxy ethylcarbamoyl-1H-1′,2′,3′-triazol-1′-yl)-*sn*-glycerol **5**), and a curcumin derivative with a terminal alkyne group (*N*-propargyl 2-(3′,5′-di (4-hydroxy-3-metoxystyryl)-1H-pyrazol-1′-yl)-acetamide **9**), as presented in synthetic Schemes 1 and 2, respectively.

For the synthesis of lipid-peg-azide **5**, compound **1** (3-azido-1,2-diol-propane) was synthesized according to the procedure of Kazemi et al. [49]; while compound **6** (9H-fluoren-9-yl)methyl prop-2-yn-1-ylcarbamate was synthesized according to the procedure reported by Seth Horne et al. [50].

Curcumin-alkyne derivative **9** was synthesized according to the procedure described in La Ferla *et al. (submitted)*.

The compound **10**, formed by click reaction between lipid-peg-azide **5** and curcumin-alkyne derivative **9** in organic media was synthesized according to Scheme 3. This new compound was used (as standard) for the determination of the yield of the click reaction on liposomes (liposomes bearing lipid-peg-azide **5** in their lipid bilayers are reacted with curcumine-alkyne **9** under click conditions, as described below).

Details about the conditions and quantities used for the synthesis of all intermediate and final compounds are reported in the Supplementary data.

### 2.3. Synthesis of curcumin-phospholipid conjugates via Michael addition

For the second preparation of curcumin-decorated nanoliposomes, a phospholipid conjugate of curcumin, 1,2-dipalmitoyl-3-(2-(1,7-bis(4-hydroxy-3-methoxyphenyl)-3,5-dioxohept-6-enylthio)ethyl phospho)-*sn*-glycerol (DPS-curcumin) **11** was synthesized via Michael addition of 1,2-Dipalmitoyl-*sn*-Glycero-3-Phosphothioethanol (Sodium Salt) [DPSH] to curcumin [51], as presented in Synthetic Scheme 4. Details about the synthesis and characterization of this compound are included in the Supplementary data.

### 2.4. Nanoliposome preparation

#### 2.4.1. Curcumin-decorated liposomes by click chemistry

Liposomes functionalized with the curcumin derivative (**9**) by the click chemistry method were prepared as described in Synthetic Scheme 5, according to the method reported recently [37,40], and more specifically to the Husigen 1,3-dipolar cycloaddition of azides and terminal alkynes [39]. In more detail, a dispersion of liposomes (DPPC/DPPG/Chol + 10–20 mol% lipid-peg-$N_3$ in PBS pH = 6.50) was added in an aqueous solution of bathophenanthrolinedisulfonate catalyst (28 mM) mixed with a pre-formed aqueous solutions of $CuSO_4$ (8 mM) and sodium ascorbate (145 mM). Then compound **9** (0.44 mg solubilized in a small volume of DMSO) was added, and the reaction was gently stirred for 8–10 h at 25–27 °C under continuous flow of $N_2$. Any aggregates that may have formed during the reaction were disaggregated by gentle bath sonication (~2–5 min) and the resulting mixture was placed in a 10.000 MW cutoff dialysis tubing (Servapore, Serva) and dialyzed against PBS buffer overnight. The vesicle dispersion was further purified by column chromatography (Sephadex 4B). Quantification of **10** in final liposomal dispersion **13** after liposomal click reaction was achieved by HPLC analysis of a specific quantity of freeze-dried liposomal dispersion and integration of the corresponding peak (see Supplementary data). HPLC was performed with a Lichrosphere 100 RP-18 (5 μm) column; eluted with a $CHCl_3$/MeOH (9:1) + 0.08% TFA mobile phase at a 1 mL/min flow rate, by a Shimatzu, LC-20AB Prominence Liquid Chromatography System.

#### 2.4.2. Curcumin decorated liposomes by curcumin-phospholipid conjugate incorporation

For the preparation of SUV DPPC/Chol(2:1) liposomes incorporating 10–20% DPS-curcumin conjugate **11**, as seen in Fig. 1, the appropriate amounts of lipids and Chol were dissolved in a chloroform/methanol (2:1 v/v) mixture, and were subsequently evaporated under vacuum until the formation of a thin lipid layer. The lipid film was treated with gas $N_2$ and was subsequently connected to a vacuum pump for 12 h, in order to remove any traces of organic solvent. The lipid film was hydrated with PBS buffer (pH 7.4) at 45 °C [or a 100 mM solution of calcein, prepared in the same buffer, in case of integrity experiments]. After complete lipid hydration and formation of liposomes, the vesicle dispersion was placed under the microtip of a probe sonicator for 10 min, or until the liposome dispersion was completely clear. The liposome dispersions were left in peace for annealing structural defects, at a temperature above the lipid transition temperature for 1–2 h.

### 2.5. Characterization of nanoparticles

#### 2.5.1. Size, polydispersity and ζ-potential

The size, polydispersity and ζ-potential of the liposome were determined using a NanoZeta series particle sizer and ζ-potential analyzer (Malvern). The size and polydispersity measurements were performed at 25 °C. Liposomes, prepared in 10 mM PBS, 150 mM NaCl, 1 mM EDTA, pH 7.4, were diluted at 0.25 mM total lipid concentration.

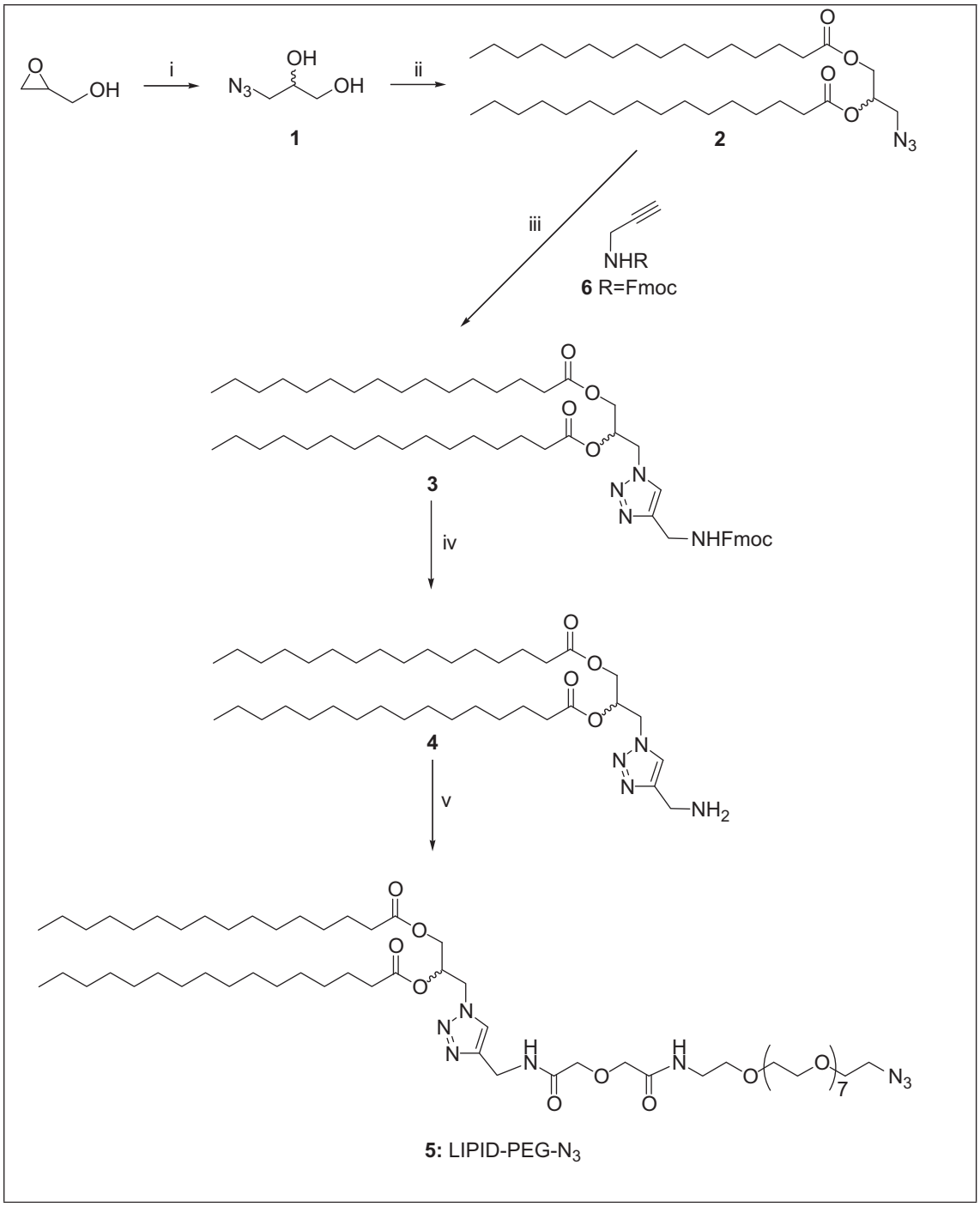


**Scheme 1.** *Reagents and Conditions*: (i) $LiBF_4$, $NaN_3$, *t*-BuOH/$H_2O$, reflux, 1 h; (ii) PalmitoylCl, Py, $CH_2Cl_2$ dry, RT, O.N., 75% over two steps; (iii) Cu(I), THF/$H_2O$, RT, O.N., 87%; (iv) Piperidine, DMF, RT, 2 h; (v) TBTU, O-(2-azidoethyl)-O'-(N-diglycolyl—2-aminoethyl) heptaethyleneglycol, DIPEA, $CH_2Cl_2$ dry, RT, 3 dd, 92%.

The particle size was assessed by dynamic laser light scattering with a 652 nm laser beam. Particle size and polydispersity index were obtained from the intensity auto-correlation function of the light scattered at a fixed angle of 173° (conditions which avoid errors due to back-scattering). The ζ-potential was measured at 25 °C. Each measurement was performed on freshly prepared liposome samples. For some of the liposome types prepared, vesicle stability was measured when the liposomes were dispersed in buffer (at various lipid concentrations) and stored at 4 °C, by following their size, polydispersity index and ζ-potential (which were measured by dynamic laser light scattering as described above) for periods of 3–30 days.

*2.5.2. Liposome integrity studies*

The integrity of vesicles with lipid membrane compositions similar to the ones used for surface decoration by the click chemistry methodology was evaluated in order to establish the optimum conditions for the reaction. Integrity of DPPC/DPPG/Chol liposomes were evaluated under the conditions and in the presence of the solutions required for the click reaction to take place. For this, the latency (%) of calcein in the vesicles was measured at various time points during incubation of liposomes at 25 or 37 °C, in presence of reaction media. Lipid/reaction compound ratios of 1:1 and 1:2 mol/mol were used. The lipid concentration in the incubated dispersions was always constant at 1 mM, and, calcein was initially encapsulated in the vesicles at a quenched concentration (100 mM). For % calcein (or CF) latency calculation [52], samples from the liposomes (20 μl) were diluted with 4 mL buffer, pH 7.40, and fluorescence intensity (FI) was measured (EX 470 nm, EM 520 nm), before and after addition of Triton X-100 at a final concentration of 1% v/v (that ensures liposome disruption and release of all encapsulated dye). Percent latency (% latency) was calculated from Eq. (1):

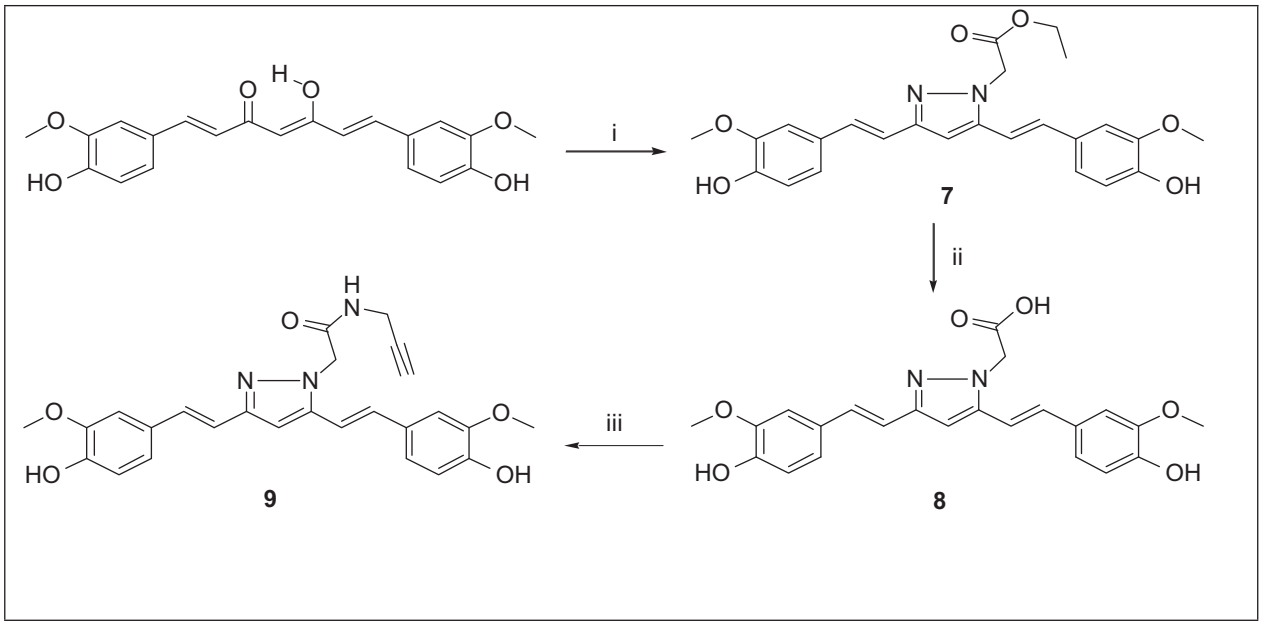


**Scheme 2.** *Reagents and Conditions*: (i) ethyl 2-hydrazinoacetate hydrochloride, TEA, toluene, reflux, O.N; (ii) KOH 1.8 M methanolic solution, RT, O.N., 87% over two steps; (iii) Propargyl amine, TBTU, HOBT, TEA, DMF dry, RT, O.N., 63%.

$$\%\ \text{Latency} = \frac{1.1\cdot(F_{AT} - F_{BT})}{1.1\cdot F_{AT}}\cdot 100 \quad (1)$$

where: $F_{BT}$ and $F_{AT}$ are calcein fluorescence intensities before and after the addition of Triton X-100, respectively.

After establishing the conditions at which the liposomes remain stable, and carrying out the click chemistry reaction for decoration of the vesicle surface as described above, the vesicles produced were studied for their integrity during incubation in absence and in presence of serum proteins. For this, liposomes that encapsulated calcein (or CF), were prepared as described above and subjected to the click reaction for curcumin attachment to their surface. They were subsequently incubated in absence or presence of serum proteins (80% v/v, FCS) and their integrity was evaluated during their incubation at 37 °C for 24 or 48 h.

### 2.6. Binding of liposomes to Aβ1-42, investigated by Surface Plasmon Resonance (SPR)

#### 2.6.1. Preparation of Aβ1-42 in different aggregation forms

A depsi-Aβ1-42 peptide was synthetized at first, as previously described [53,54]. This depsi-peptide is much more soluble than the native peptide and it also has a much lower propensity to aggregate, so preventing the spontaneous formation of 'seeds' in solution. The native Aβ1-42 peptide was then obtained from the depsi-peptide by a "switching" procedure involving a change in pH [53–55]. The Aβ1-42 peptide solution obtained immediately after switching is seed-free as shown in carefully conducted previous work [54,55]. The Aβ1-42 peptide obtained with this procedure is therefore in its very initial state and, for sake of simplicity it will be referred to here as "monomers".

To prepare Aβ1-42 fibrils, the switched peptide solution was diluted with water to 100 μM, acidified to pH 2.0 with 1 M HCl, and left to incubate for 24 h at 37 °C [56]. Kinetic studies with circular dicroism and thioflavin-T clearly indicated that these conditions enable to reach the maximal level of β-sheet structures whereas the presence of amyloid fibrils was directly confirmed by atomic force microscopy (AFM) [55].

#### 2.6.2. Surface Plasmon Resonance (SPR) analysis

For these studies we used the ProteOn XPR36 (Biorad) apparatus, which has six parallel flow channels that can be used to uniformly immobilize strips of six "ligands" on the sensor surface. Aβ1-42 "monomers" or fibrils were immobilized in two of these parallel-flow channels of a GLC sensor chip (Biorad) using amine-coupling chemistry. Briefly, after surface activation the peptide solutions (10 μM in acetate buffer pH 4.0) were injected for 5 min at a flow rate of 30 mL/min, and the remaining activated groups were blocked with ethanolamine, pH 8.0. Bovine serum albumin (BSA) was also immobilized in another parallel flow channel, as a reference protein. The final immobilization levels were similar, about 2500 Resonance Units (1 RU = 1 pg protein/mm$^2$). A fourth surface was prepared using the same immobilization procedure but without addition of the peptide ("empty", reference surface).

The fluidic system of Proteon XPR36 can automatically rotate 90° so that up to six different "analytes" (e.g. different liposome preparations, or different concentrations of the same preparation) could be injected simultaneously over all the different immobilized molecules [57].

Preliminary injections were done in order to check for the binding features of the immobilized Aβ species. We thus injected the anti-Aβ antibody 4G8 (Covance) which, as expected bound to both Aβ fibrils and "monomers" (not shown) whereas

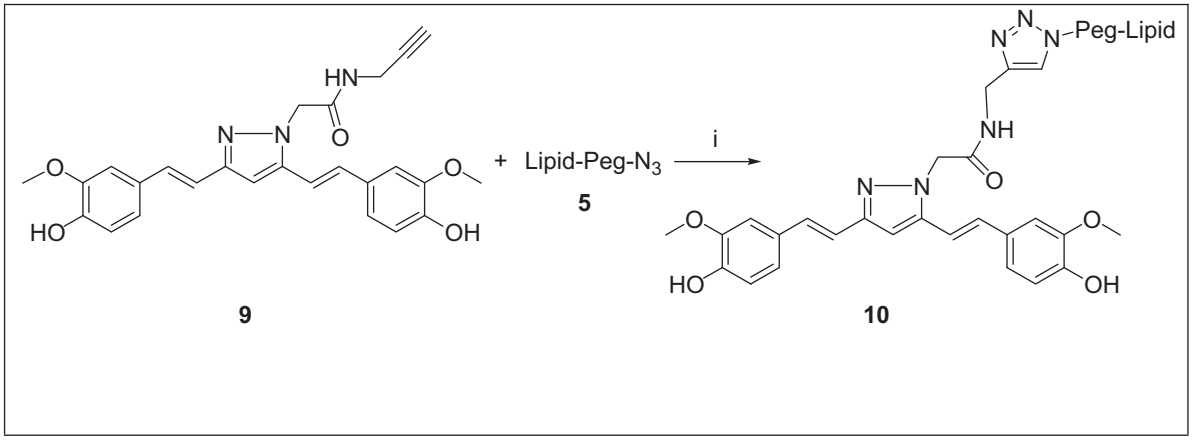


**Scheme 3.** *Reagents and Conditions*: (i) Procedure A: $CuSO_4\cdot 5H_2O$, sodium ascorbate, THF–$H_2O$, RT, 87%; Procedure B: CuBr, PMDTA, sodium ascorbate, AcCN–$H_2O$, RT, 10 min, 92%.

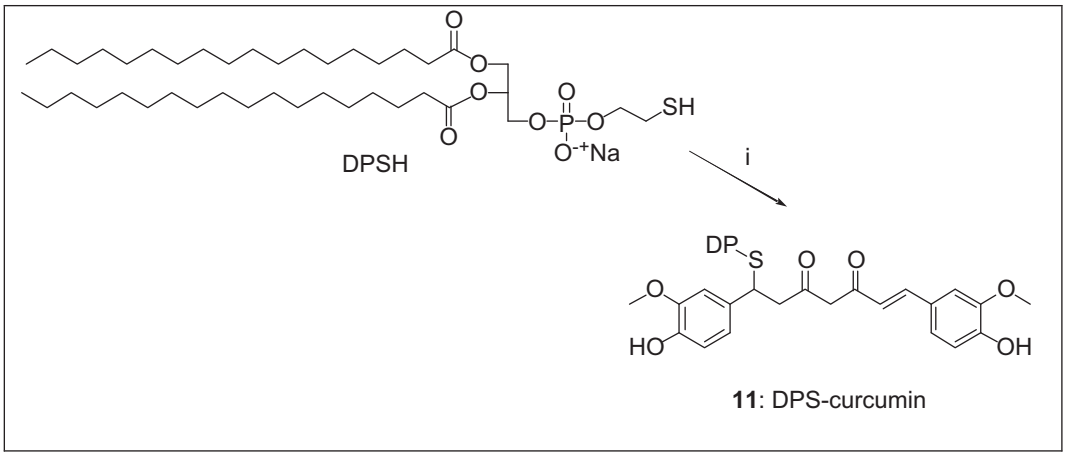


**Scheme 4.** *Reagents and Conditions*: (i) Curcumin, $CH_2Cl_2$, DIPEA, R.T., O.N., 75%.

Congo-Red, a dye specifically recognizing β-sheet-containing species, only bound to Aβ fibrils but not "monomers" (not shown).

ProteOn analysis software (BioRad) was used for the fitting of sensorgrams, to obtain the association and dissociation rate constants of the binding ($K_{on}$ and $K_{off}$) and the corresponding $K_D$ value. The simplest 1:1 interaction model (Langmuir model) is used at first.

## 3. Results

### 3.1. Preparation of curcumin-decorated nanoliposomes by click chemistry

#### 3.1.1. Integrity of liposomes during the click reaction

Before using pre-formed liposomes for the click chemistry reaction, their integrity during incubation in presence of the required chemicals was investigated. As seen in Fig. 2, when the incubation was done at 37 °C (Fig. 2A) the liposomes were not stable, since the liposome encapsulated dye (calcein) leaked out of the vesicles, at significant amounts even during the first 2–3 h of incubation, while approximately 50% of the vesicle-encapsulated dye was released after 6 h of incubation. This result suggests that the click reaction should not be carried out on liposomes (with this lipid composition) at 37 °C. Oppositely, at 25 °C the liposomes are stable for the first 6 h of incubation in presence of the reactants required for the click reaction to take place (Fig. 2B) and also in presence of double amounts of reactants. Even after 24 h incubation at room temperature the vesicle are more or less stable, since the percent of dye released is very low. This proves that it is important to carry out the reaction at room temperature and not at 37 °C, especially when valuable drug molecules are entrapped in the vesicles, before the click reaction takes place.

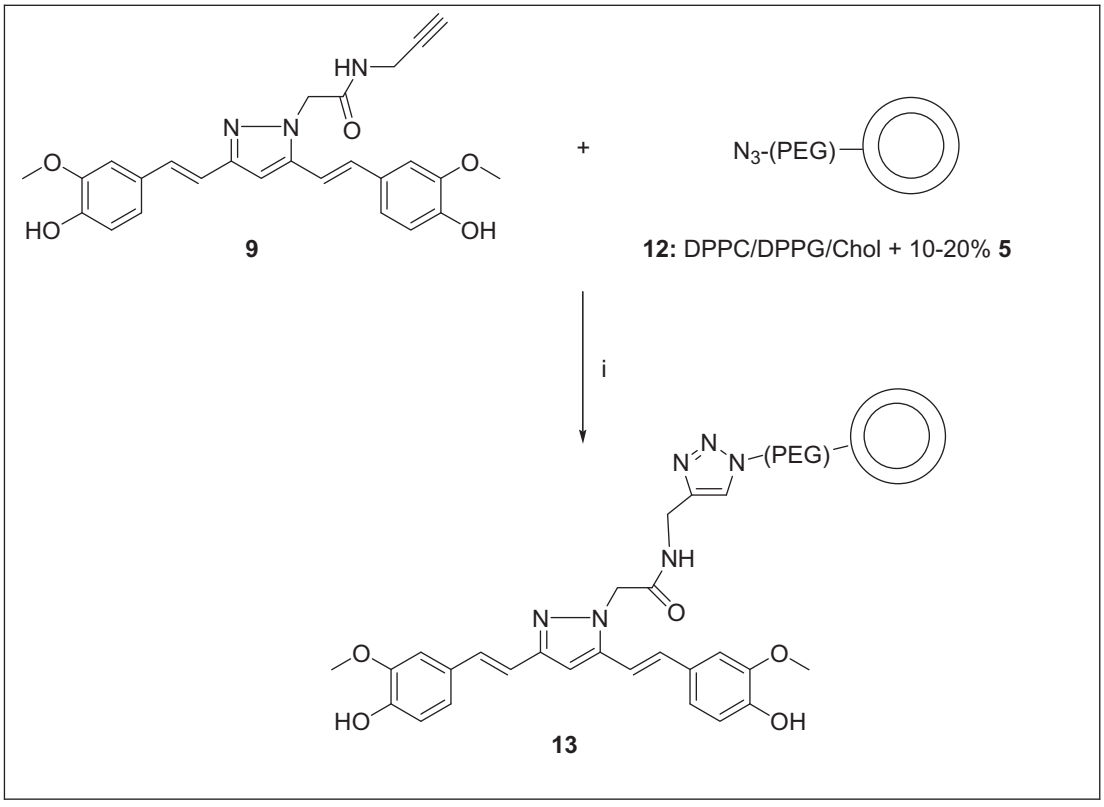


**Scheme 5.** *Reagents and Conditions*: (i) $CuSO_4 \cdot 5H_2O$, sodium ascorbate, bathophenanthrolinedisulfonate, buffer PBS 6,5, $N_2$, R.T., 6–8 h.

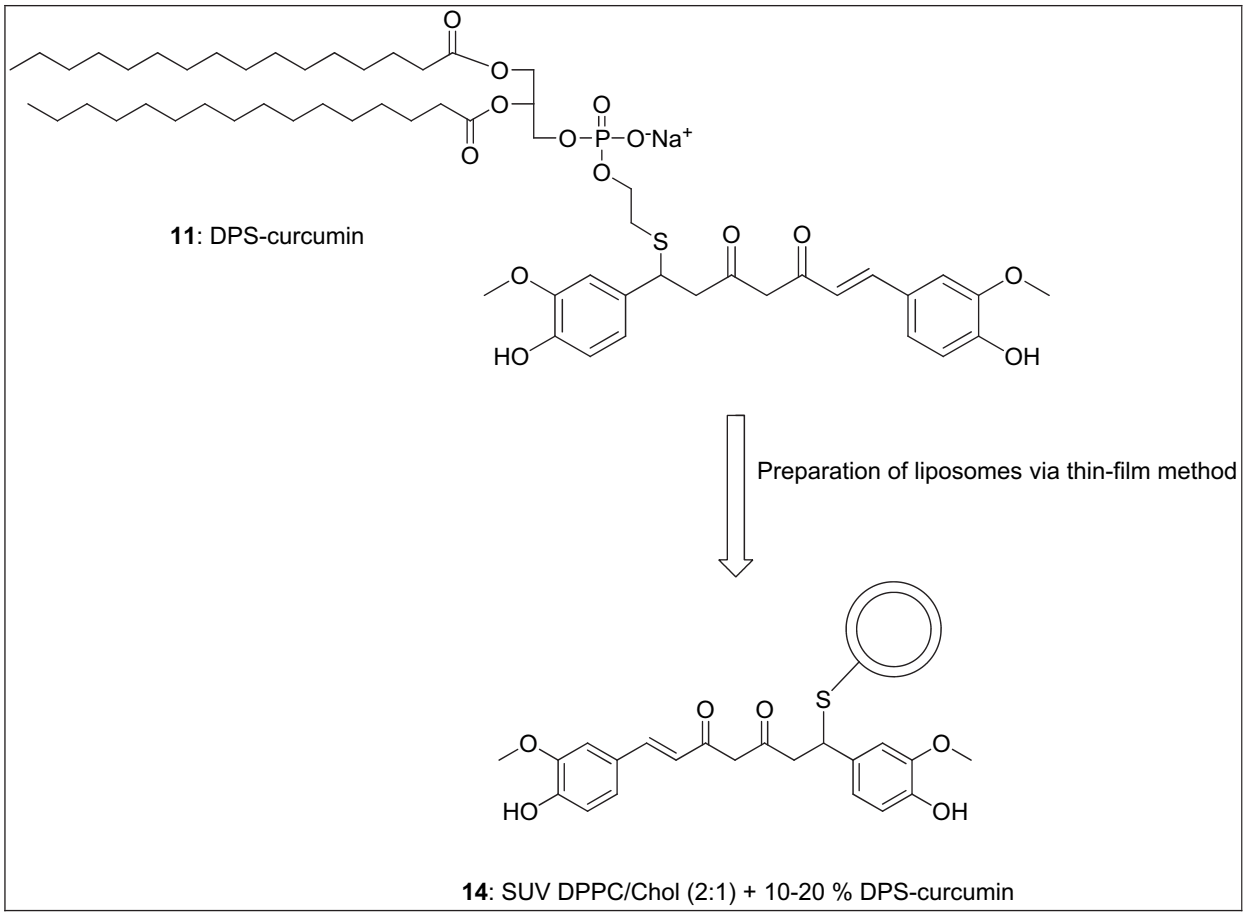


**Fig. 1.** Formation of curcumin-decorated nanoliposomes by incorporation of the phospholipid conjugate of curcumin (compound **11**) in liposome membrane prepared by the thin film-hydration method.

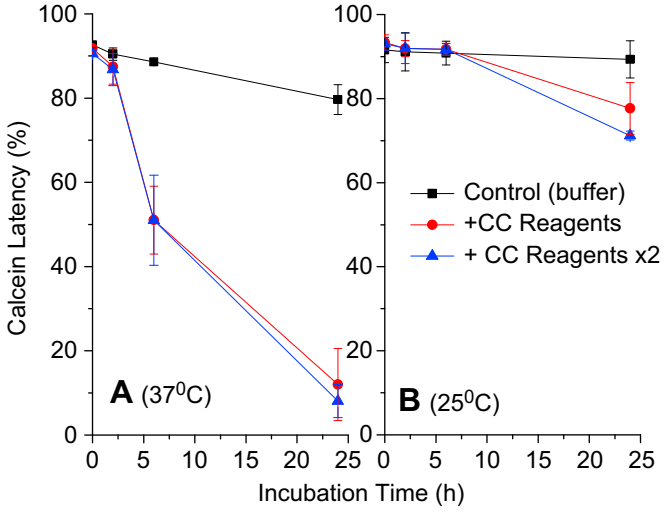


**Fig. 2.** Integrity of liposomes (DPPC/DPPG/Chol 8:2:5), expressed as latency of vesicle-encapsulated calcein, during incubation in PBS buffer (control) or in presence of the reagents required for the click chemistry reaction to take place. Vesicle integrity was studied in presence of the normal quantities of reagents required, as mentioned analytically in the Methods section (CC Reagents) or in presence of double amounts (x2 CC Reagents), at 37 °C (graph A) or 25 °C (graph B). Each data point is the mean of at least 3 different experiments and the bar is the SD of the mean.

*3.1.2. Confirmation of compound identity – yield of click chemistry reaction – liposomes **13***

Final confirmation that the click reaction is indeed taking place and liposomes **13** are forming, was provided by identification of the presence of compound **10** in the liposome dispersion after liposomal breakage and HPLC analysis of the resulting mixture (for more details, HPLC and ESI-MS graphs see Supplementary Data). The yield of the click reaction was determined by quantifying the amount of product **10** in weighted quantities of freeze-dried liposomal dispersions, and proved to range between 75 and 95 percent.

*3.2. Physicochemical properties of liposomes*

The mean diameters and ζ-potential values measured for the various types of nanoliposomes prepared are presented in Table 1. As seen, vesicle size increases as a function of the percent of curcumin decoration on the vesicle surface, for both liposomes **13** and liposomes **14**. In all cases, the polydispersity indices measured were low (ranging from 0.097 to 0.255) indicating that the nanoliposomes prepared have very narrow size distributions. The surface charge of curcumin-decorated vesicles is negative in all cases, indicating that curcumin on the surface influences the ζ-potential of the vesicles, which is normal if considering that curcumin has two phenol groups which are partly ionized at pH 7.40.

*3.3. Vesicle size stability and integrity studies*

The stability (mean diameter and ζ-potential values) of two different preparations of liposomes **13** [having different amounts of

**Table 1**
Physicochemical characteristics of the various liposome types prepared, depending on the percent (theoretical) of curcumin present on the vesicle surface. Vesicle mean diameter (in nm), Polydispersity index and ζ-potential (in mV) are measured, as described in the methods section and values reported are the mean values from at least 5 measurements of 3 different preparations, in each case.

| Liposome type | Percent surface curcumin (mol%) | Mean diameter (nm) | Polydispersity index (PI) | ζ-Potential (mV) |
|---|---|---|---|---|
| **Liposome 13 -CONTROL** | 0 | 52.8 ± 5.5 | 0.097 | −7.6 ± 1.7 |
| **Liposome 13** | 5 | 130.9 ± 1.1 | 0.108 | −24.30 ± 0.42 |
| **Liposome 13** | 10 | 168.9 ± 1.3 | 0.164 | −20.3 ± 1.4 |
| **Liposome 14 - CONTROL** | 0 | 63.1 ± 6.2 | 0.195 | −6.44 ± 0.49 |
| **Liposome 14** | 1 | 135.30 ± 0.70 | 0.209 | – |
| **Liposome 14** | 5 | 180 ± 13 | 0.193 | −14.5 ± 2.4 |
| **Liposome 14** | 10 | 207.2 ± 8.0 | 0.255 | −10.5 ± 1.2 |

curcumin on their surface], during storage at 4 °C, for a period of 15 days is presented in Fig. 3. As seen, both liposome preparations are very stable for the storage period in terms of size distribution and surface charge value. No signs of liposome aggregation was evident when the liposomes were stored dispersed at the specific lipid concentrations used herein (up to 5 mg/mL). Liposomes **14** were also found to be stable under identical conditions, for more than 20 days of storage (results not shown).

The integrity of selected types of liposomes **13** and **14**, during incubation in presence of serum proteins is presented in Fig. 4 (A & B, respectively). In both cases, the integrity of control liposomes (that have the same lipid composition but no curcumin on their surface) are also studied in parallel, while both types of liposomal dispersions (control and curcumin-decorated) are also incubated in presence of plain buffer for comparison. As seen, both liposome types are equally stable when compared with the relevant control liposomes, during incubation in buffer, as well as in the presence of FCS, for a period of at least 24 h, indicating that these liposomes posses the required stability for in vivo applications.

In the case of liposomes **13**, the control liposomes were actually the same liposomes before the click reaction step was carried out. This result proves that under the specific conditions applied,

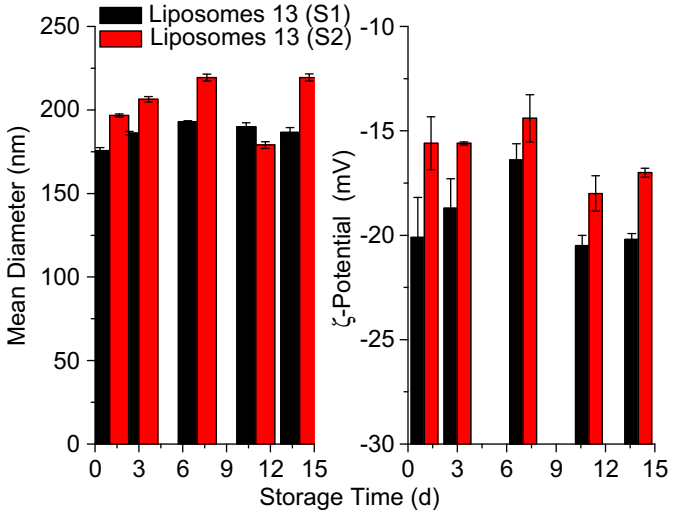


**Fig. 3.** Size (d-hydrodynamic diameter, nm) and ζ-Potential values of two different vesicle batches of liposomes **13** (decorated with 5 mol% [S1] or 10 mol% [S2] curcumin), dispersed in PBS buffer at a lipid concentration of 10–15 mg/mL, during storage at 4 °C. Each value is the mean of at least 5 different measurements and bars are the SD values of each mean.

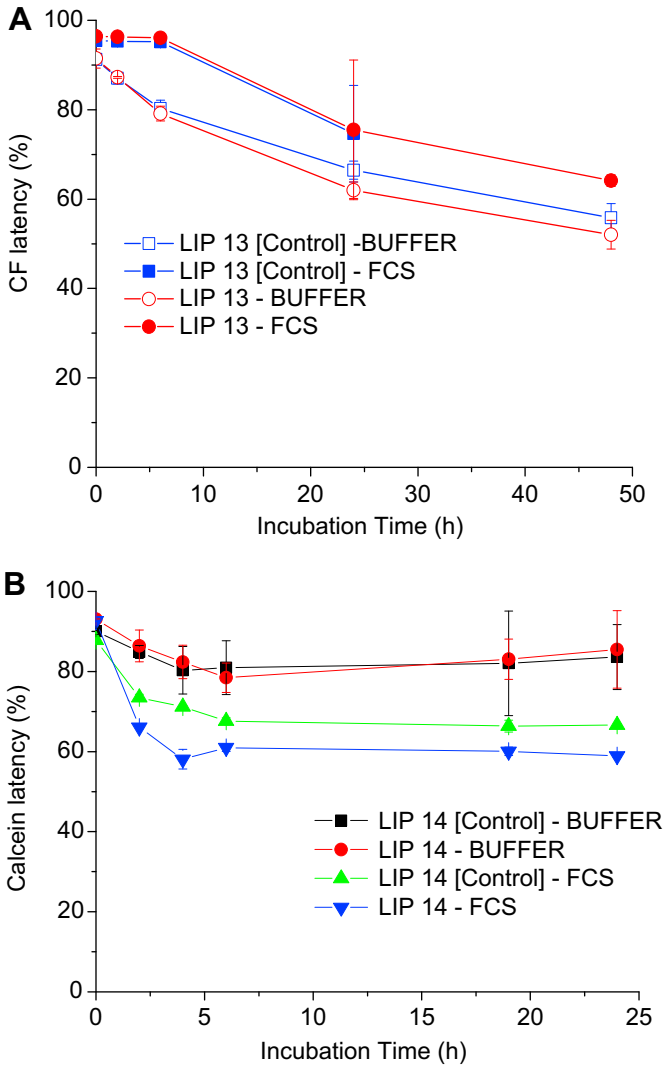


**Fig. 4.** Integrity of liposomes **13** (A) and **14** (B) and their corresponding control liposomes (with no curcumin on their surface), during incubation in buffer or FCS (80% v/v) at 37 °C. Each data point is the mean of at least 3 different experiments and the bar is the SD of the mean.

liposomes which are pre-formed to encapsulate active drugs or other types of bioactive molecules can be subjected to click reaction and after appropriate purification, they can be used for in vivo applications.

### 3.4. Binding of functionalized liposomes to Aβ1-42

Before using compound **9** for preparation of curcumin-decorated liposomes **13**, its affinity for Aβ1-42 fibrils was confirmed by SPR studies, using a derivative of compound **9** obtained via click reaction with a short PEG chain. The results of this initial confirmatory experiment are presented in the Supplementary data (Section S2, Fig. S1).

Liposomes **13** and **14** , as well as plain, i.e. not functionalized, liposomes were flowed over parallel flow channels of the same sensor chip immobilizing Aβ1-42 fibrils, Aβ1-42 “monomers”, BSA (to check the specificity of the interaction), and nothing (empty surface).

No binding was detected when using plain liposomes, as well as liposomes **14** on the four sensor surfaces, even at highest curcumin concentrations (light blue lines, Fig. 5). On the contrary, liposomes

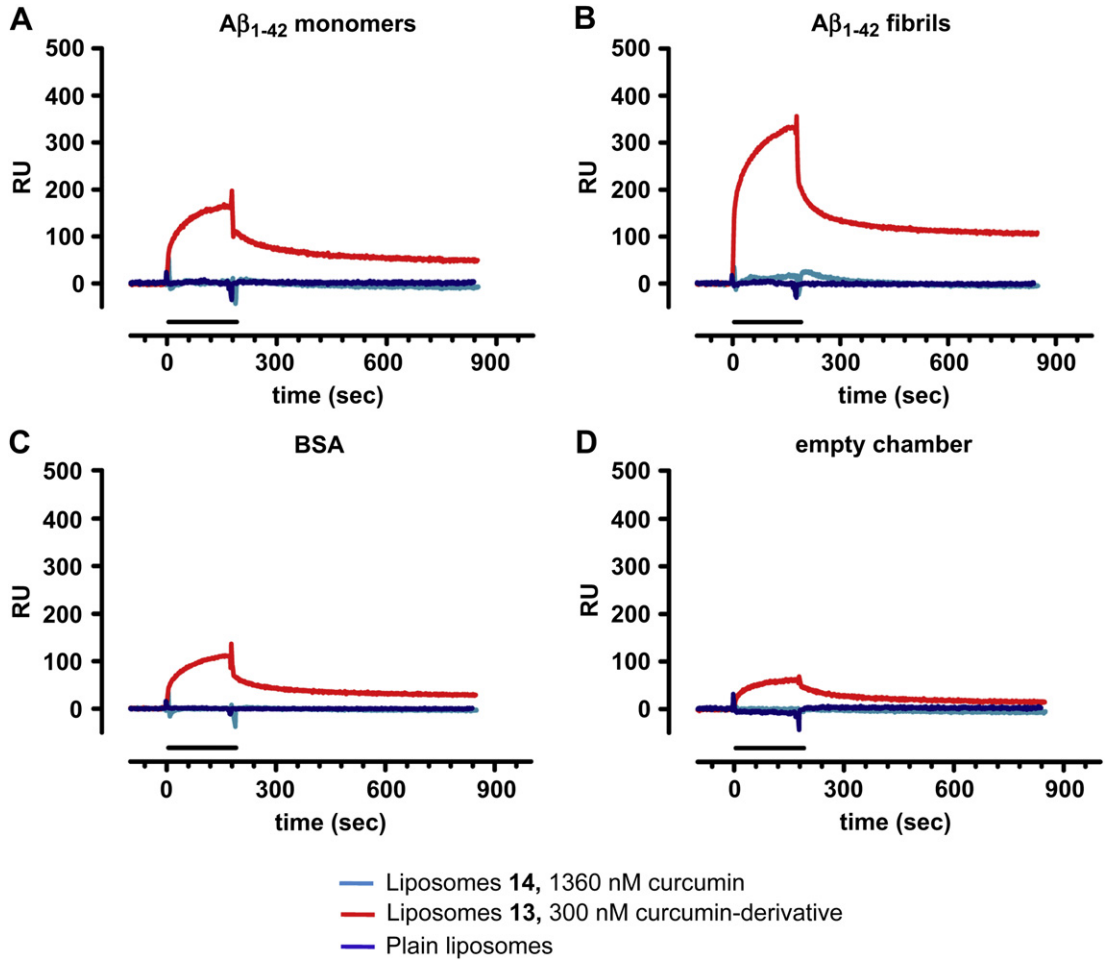


**Fig. 5.** SPR studies comparing the binding properties of liposomes **13**, liposomes **14** and plain liposomes when injected onto sensor surfaces immobilizing Aβ1-42 monomers (A), Aβ1-42 fibrils (B) or bovine serum albumin (BSA) (C), at similar densities; panel D refers to the signal measured in the reference, empty, surface. The figure shows representative sensorgrams (resonance units, RU, versus time) obtained by simultaneous injection of the different liposomes, for 3 min (as indicated) over all the sensor chip surfaces. Liposomes **13** (red) were injected at a concentration corresponding to 300 nM of exposed curcumin derivative; liposomes **14** (light blue), as well as plain liposomes (dark blue) were injected at a concentration corresponding to 1360 nM of exposed curcumin.

**13** interacted with immobilized Aβ1-42 species (red lines, Fig. 5A and B), in particular with Aβ1-42 fibrils (Fig. 5B). A lower binding was observed on BSA (Fig. 5C) and an even lower binding was detected on empty surface (Fig. 5D).

Fig. 6 shows the concentration-dependence of the specific binding of liposomes **13** to immobilized Aβ1-42 fibrils, i.e. after correction of the signal measured in the reference surface. For these experiments, in particular, we used liposomes with a different density of surface functionalization (5 or 10%, see Materials and Methods) and injected three concentrations of each of them, to have 100, 300 and 600 nM of exposed curcumin derivative. The resulting sensorgrams, shown in Fig. 6, could not be fitted by a simple 1: 1 interaction model (Langmuir equation) but require more complex interaction models. This is clearly evident by the dissociation phase which cannot be fitted by a mono-exponential curve (as expected for simple interactions), indicating at least two binding components with two different rate constants, one faster and one slower. The fitting of these sensorgrams with a "two-site" model is shown as white lines in Fig. 6, and allowed to estimate the binding constants of the two putative components, highlighting in particular the presence of a component representing about 40% of the binding and characterized by a very low dissociation rate constants ($<3 \times 10^{-4}$ $s^{-1}$, pseudo-irreversible binding) (Fig. 6). The corresponding $K_D$ values of the exposed curcumin derivative was calculated to be in the low nM range (2–10 nM). Importantly, the sensorgrams obtained with the different concentrations could not be globally fitted, suggesting that even the binding to this high affinity component is complex and likely involve avidity effects [58].

## 4. Discussion

Curcumin-decorated liposomes were prepared and studied for their integrity, stability and binding affinity to Aβ1-42 fibrils. For preparation of curcumin-decorated vesicles **13**, a click chemistry method was used, after an appropriate curcumin derivative **9** was synthesized. Initial vesicle integrity experiments revealed that the click chemistry reaction should be carried out at room temperature (Fig. 2B), since at 37 °C the liposome integrity is highly affected (Fig. 2A) by the reaction media required for the click to occur [44]. Of course this is the case for the specific liposomes (with lipid composition of DPPC/DPPG/Chol 8:2:5 mol/mol/mol) evaluated herein; perhaps other lipid compositions may be more or less stable; in the last case perhaps it would be required to use milder conditions for click attachment [59] (in order to preserve vesicle integrity during the reaction to decorate their surface). For construction of liposomes as negative controls, a second method

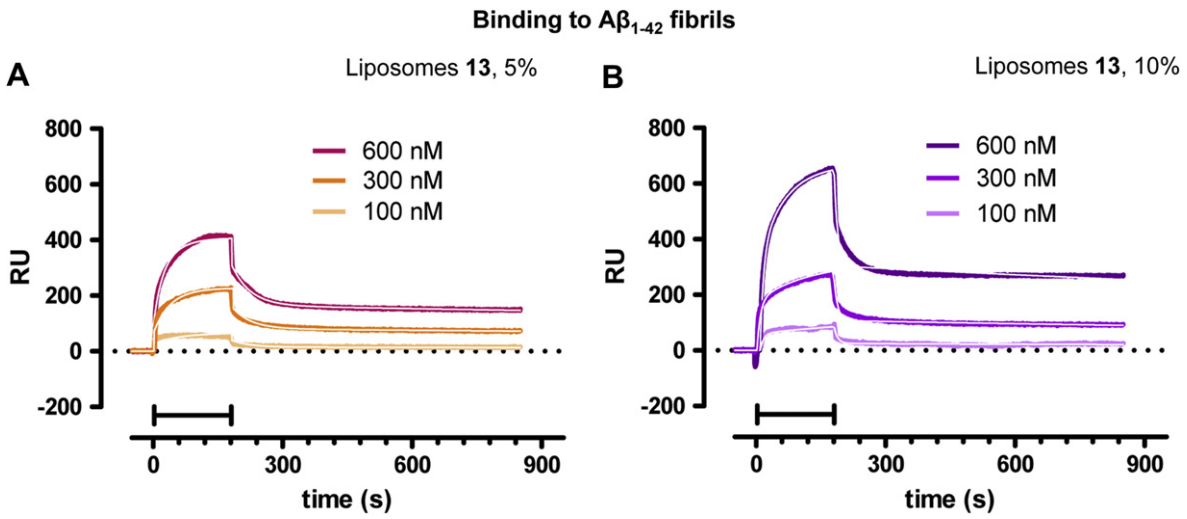


**Fig. 6.** Concentration-dependent binding of liposomes **13** to Aβ1-42 fibrils immobilized on the SPR sensor chip. For this session, liposomes with two different densities of functionalization with the curcumin derivative (5 and 10%) were used. Liposomes were injected at concentrations corresponding to 100, 300 and 600 nM of exposed curcumin derivative. The figure shows representative sensorgrams (resonance units, RU, versus time) obtained by simultaneous injection of the liposomes, for 3 min over sensor chip surfaces (as indicated). The reported sensorgrams are indicative of a specific binding to Aβ1-42, since they were obtained after subtraction of the signal detected in the reference surface, thus correcting for binding-independent responses, such as bulk effects due to buffer exchanges or drift effects. The fitting of these sensorgrams, with a "two-sites" model, are shown in white.

was also used for attachment of curcumin on the surface of vesicles (liposomes **14**), in which case the planar structure of curcumin, required for its activity [34], is disrupted.

Both techniques utilized herein for formation of curcumin-decorated nanosized liposomes were successful to prepare nanosized liposomes (Table 1) with the appropriate stability to be used for in vivo applications (Figs. 2 and 3) and high stability during storage (Fig. 4). As the amount of curcumin molecules attached to the vesicle surface increases, the vesicles produced (by both techniques evaluated) demonstrated an increase in mean diameter (as anticipated due to the curcumin coating), however the vesicle population was still homogeneous, as judged by the low polydispersity indices of the dispersions (Table 1).

SPR binding results (Fig. 5) show that the liposomes **14** on which curcumin was attached without preservation of its structural planarity, do not show any binding affinity to the immobilized Aβ1-42 fibrils; whereas the vesicles exposing a curcumin derivative maintaining the planarity showed very high binding. This result proves that this specific structural characteristic is indeed required for curcumin binding to the fibrils. Furthermore, the current results enhance the opinion that curcumin derivatives exist predominantly in the enol form during binding to Aβ aggregates, and that the enolization of curcumin derivatives is crucial for binding to Aβ aggregates [60].

In more detail, the curcumin derivative **9** showed a clear binding to immobilized Aβ1-42 fibrils, with an estimated $K_D$ value of 7 μM, whereas a lower binding was detected on Aβ1-42 "monomers". In particular, while all the binding to "monomers" has a very fast dissociation rate, a significant amount of binding to fibrils dissociates very slowly, indicating a more persistent interaction.

Interestingly, the affinity of the curcumin derivative - exposed on liposomes 13 – for Abeta fibrils (2–10 nM) was much higher than the affinity of a corresponding compound not attached to liposomes (7 uM, see Supplementary data). We suggest the involvement of multivalent interactions, i.e. different molecules of curcumin derivative on the same liposome contribute to the binding to the immobilized Aβ1-42 fibrils. It has been previously shown, in fact, that a multivalent ligand (dendrimer [40]; nanoparticle [41]) has a binding affinity for its target which can greatly exceed, even by 2–3 orders of magnitude, the binding affinity of the same ligand, if monovalent. This increase of affinity was due, in particular, to a decrease of the dissociation rate constants, approaching those of a pseudo-irreversible binding, and the same finding was actually found with our liposomes decorated with the curcumin derivatives. The binding of the decorated liposomes for BSA was much lower and this is consistent with the lack of binding of the curcumin derivative for this plasmatic protein.

## 5. Conclusions

The click chemistry methodology was successfully utilized for decoration of the surface of nanoliposomes with a curcumin derivative which retains the structural characteristics required for the antifibrillogenic activity. These nanosized curcumin-decorated liposomes showed the highest affinity for Aβ1-42 fibrils (1–5 nM) reported up-to-date and sufficient integrity/stability for in vivo applications. Thus, they are potentially very useful in the attempt to target these AD pathogenic markers for diagnostic and/or therapeutic purposes.

## Funding

Funding source had no involvement in study design; in the collection, analysis, and interpretation of data; in the writing of the report; and in the decision to submit the paper for publication.

## Acknowledgements

The research leading to these results has received funding from the European Community's Seventh Framework Programme (FP7/2007-2013) under grant agreement no. 212043.

## Appendix. Supplementary data

Supplementary data related to this article can be found online at doi:10.1016/j.biomaterials.2010.10.027.

## Appendix

Figure with essential color discrimination. Figs. 2–6, in this article is difficult to interpret in black and white. The full color images can be found in the online version, at doi:10.1016/j.biomaterials.2010.10.027.

## References


[1] Brookmeyer R, Gray S, Kawas C. Projections of Alzheimer's disease in the United States and the public health impact of delaying disease onset. Am J Public Health 1998;88(9):1337–42.
[2] American Health Assistance Foundation. Alzheimer disease research: about Alzheimer, http://wwwahaforg/alzheimers/about/2000-2010.
[3] Brookmeyer R, Corrada MM, Curriero FC, Kawas C. Survival following a diagnosis of Alzheimer disease. Arch Neurol 2002;59(11):1764–7.
[4] Ferri CP, Prince M, Brayne C, Brodaty H, Fratiglioni L, Ganguli M, et al. Global prevalence of dementia: a Delphi consensus study. Lancet 2005;366(9503):2112–7.
[5] Alzheimer Europe and Eurostat, www.AlzheimerEurope.org.
[6] Citron M. Alzheimer's disease: strategies for disease modification. Nat Rev Drug Discov 2010;9(5):387–98.
[7] Mann DM, Iwatsubo T, Ihara Y, Cairns NJ, Lantos PL, Bogdanovic N, et al. Predominant deposition of amyloid-beta 42(43) in plaques in cases of Alzheimer's disease and hereditary cerebral hemorrhage associated with mutations in the amyloid precursor protein gene. Am J Pathol 1996;148(4):1257–66.
[8] Selkoe DJ. Alzheimer's disease: genes, proteins, and therapy. Physiol Rev 2001;81(2):741–66.
[9] Siemers E, DeMattos RB, May PC, Dean RA. Role of biochemical Alzheimer's disease biomarkers as end points in clinical trials. Biomark Med 2010;4(1):81–9.
[10] Yin YI, Bassit B, Zhu L, Yang X, Wang C, Li YM. {gamma}-secretase substrate concentration modulates the abeta42/abeta40 ratio: implications for Alzheimer disease. J Biol Chem 2007;282(32):23639–44.
[11] Barnham KJ, Masters CL, Bush AI. Neurodegenerative diseases and oxidative stress. Nat Rev Drug Discov 2004;3(3):205–14.
[12] Lambert MP, Barlow AK, Chromy BA, Edwards C, Freed R, Liosatos M, et al. Diffusible, nonfibrillar ligands derived from abeta1-42 are potent central nervous system neurotoxins. Proc Natl Acad Sci U S A 1998;95(11):6448–53.
[13] Cleary JP, Walsh DM, Hofmeister JJ, Shankar GM, Kuskowski MA, Selkoe DJ, et al. Natural oligomers of the amyloid-beta protein specifically disrupt cognitive function. Nat Neurosci 2005;8(1):79–84.
[14] Walsh DM, Selkoe DJ. A beta oligomers – a decade of discovery. J Neurochem 2007;101(5):1172–84.
[15] Haass C, Selkoe DJ. Soluble protein oligomers in neurodegeneration: lessons from the Alzheimer's amyloid beta-peptide. Nat Rev Mol Cell Biol 2007;8(2):101–12.
[16] Carrell RW, Mushunje A, Zhou A. Serpins show structural basis for oligomer toxicity and amyloid ubiquity. FEBS Lett 2008;582(17):2537–41.
[17] Pahnke J, Walker LC, Scheffler K, Krohn M. Alzheimer's disease and blood-brain barrier function-why have anti-beta-amyloid therapies failed to prevent dementia progression? Neurosci Biobehav Rev 2009;33(7):1099–108.
[18] Dasilva KA, Shaw JE, McLaurin J. Amyloid-beta fibrillogenesis: structural insight and therapeutic intervention. Exp Neurol 2010;223(2):311–21.
[19] Findeis MA. The role of amyloid beta peptide 42 in Alzheimer's disease. Pharmacol Ther 2007;116(2):266–86.
[20] De Felice FG, Ferreira ST. Beta-amyloid production, aggregation, and clearance as targets for therapy in Alzheimer's disease. Cell Mol Neurobiol 2002;22(5–6):545–63.
[21] Greenberg SM, Grabowski T, Gurol ME, Skehan ME, Nandigam RN, Becker JA, et al. Detection of isolated cerebrovascular beta-amyloid with Pittsburgh compound B. Ann Neurol 2008;64(5):587–91.
[22] Look GC, Jerecic J, Cherbavaz DB, Pray TR, Breach JC, Crosier WJ, et al. Discovery of ADDL–targeting small molecule drugs for Alzheimer's disease. Curr Alzheimer Res 2007;4(5):562–7.
[23] Matsuoka Y, Saito M, LaFrancois J, Gaynor K, Olm V, Wang L, et al. Novel therapeutic approach for the treatment of Alzheimer's disease by peripheral administration of agents with an affinity to beta-amyloid. J Neurosci 2003;J23(1):29–33.
[24] Sagare A, Deane R, Bell RD, Johnson B, Hamm K, Pendu R, et al. Clearance of amyloid-beta by circulating lipoprotein receptors. Nat Med 2007;13(9):1029–31.
[25] Shen Y, Yu LC. Potential protection of curcumin against hypoxia-induced decreases in beta-III tubulin content in rat prefrontal cortical neurons. Neurochem Res 2008;33(10):2112–7.
[26] Zhao BL, Li XJ, He RG, Cheng SJ, Xin WJ. Scavenging effect of extracts of green tea and natural antioxidants on active oxygen radicals. Cell Biophys 1989;14(2):175–85.
[27] Thomas T, Nadackal TG, Thomas K. Aspirin and non-steroidal anti-inflammatory drugs inhibit amyloid-beta aggregation. Neuroreport 2001;12(15):3263–7.
[28] Ono K, Hasegawa K, Naiki H, Yamada M. Curcumin has potent anti-amyloidogenic effects for Alzheimer's beta-amyloid fibrils in vitro. J Neurosci Res 2004;M75(6):742–50.
[29] Kim H, Park BS, Lee KG, Choi CY, Jang SS, Kim YH, et al. Effects of naturally occurring compounds on fibril formation and oxidative stress of beta-amyloid. J Agric Food Chem 2005;53(22):8537–41.
[30] Yang F, Lim GP, Begum AN, Ubeda OJ, Simmons MR, Ambegaokar SS, et al. Curcumin inhibits formation of amyloid beta oligomers and fibrils, binds plaques, and reduces amyloid in vivo. J Biol Chem 2005;280(7):5892–901.
[31] Kim DS, Park SY, Kim JK. Curcuminoids from curcuma longa L. (zingiberaceae) that protect PC12 rat pheochromocytoma and normal human umbilical vein endothelial cells from abeta(1–42) insult. Neurosci Lett 2001;303(1):57–61.
[32] Re F, Airoldi C, Zona C, Masserini M, La Ferla B, Quattrocchi N, et al. Beta amyloid aggregation Inhibitors: small molecules as candidate drugs for therapy of Alzheimer's disease. Curr Med Chem; 2010 [Epub ahead of print].
[33] Ganguli M, Dodge HH, Chen P, Belle S, DeKosky ST. Ten-year incidence of dementia in a rural elderly US community population: the MoVIES project. Neurology 2000;54(5):1109–16.
[34] Reinke AA, Gestwicki JE. Structure–activity relationships of amyloid beta-aggregation inhibitors based on curcumin: influence of linker length and flexibility. Chem Biol Drug Des 2007;70(3):206–15.
[35] Anand P, Thomas SG, Kunnumakkara AB, Sundaram C, Harikumar KB, Sung B, et al. Biological activities of curcumin and its analogues (congeners) made by man and mother nature. Biochem Pharmacol 2008;76(11):1590–611.
[36] Bernabe-Pineda M, Ramirez-Silva MT, Romero-Romo M, Gonzalez-Vergara E, Rojas-Hernandez A. Determination of acidity constants of curcumin in aqueous solution and apparent rate constant of its decomposition. Spectrochim Acta A Mol Biomol Spectrosc 2004;60(5):1091–7.
[37] Wang YJ, Pan MH, Cheng AL, Lin LI, Ho YS, Hsieh CY, et al. Stability of curcumin in buffer solutions and characterization of its degradation products. J Pharm Biomed Anal 1997;15(12):1867–76.
[38] Tonnesen HH, Karlsen J. Studies on curcumin and curcuminoids. VI. Kinetics of curcumin degradation in aqueous solution. Z Lebensm Unters Forsch 1985;180(5):402–4.
[39] Montet X, Funovics M, Montet-Abou K, Weissleder R, Josephson L. Multivalent effects of RGD peptides obtained by nanoparticle display. J Med Chem 2006;49(20):6087–93.
[40] Hong S, Leroueil PR, Majoros IJ, Orr BG, Baker Jr JR, Banaszak Holl MM. The binding avidity of a nanoparticle-based multivalent targeted drug delivery platform. Chem Biol 2007;14(1):107–15.
[41] Tassa C, Duffner JL, Lewis TA, Weissleder R, Schreiber SL, Koehler AN, et al. Binding affinity and kinetic analysis of targeted small molecule-modified nanoparticles. Bioconjug Chem 2010;21(1):14–9.
[42] Antimisiaris SG, Kallinteri P, Fatouros D. Liposomes and drug delivery. In: Gad SC, editor. Pharmaceutical manufacturing handbook production and processes. John Wiley & Sons; 2008. p. 443–533.
[43] Said Hassane F, Frisch B, Schuber F. Targeted liposomes: convenient coupling of ligands to preformed vesicles using "click chemistry. Bioconjug Chem 2006;17(3):849–54.
[44] Cavalli S, Tipton AR, Overhand M, Kros A. The chemical modification of liposome surfaces via a copper-mediated [3 + 2] azide-alkyne cycloaddition monitored by a colorimetric assay. Chem Commun (Camb) 2006;30:3193–5.
[45] Hein CD, Liu XM, Wang D. Click chemistry, a powerful tool for pharmaceutical sciences. Pharm Res 2008;25(10):2216–30.
[46] Frisch B, Hassane FS, Schuber F. Conjugation of ligands to the surface of preformed liposomes by click chemistry. Methods Mol Biol 2010;605:267–77.
[47] Thoma K, Rombach R, Ullmann E. Thin-layer chromatographic differentiation of homologous polyethylene glicols. Sci Pharm 1964;32:216–24.
[48] Dittmer JC, Lester RL. A simple, specific spray for the detection of phospholipids on thin-layer chromatograms. J Lipid Res 1964;15:126–7.
[49] Kazemi F, Kiasat AR, Ebrahimi S. Regioselective azidolysis of epoxides catalyzed with $LiBF_4$. Synth Commun 2003;33:999–1004.
[50] Horne WS, Stout CD, Ghadiri MR. A heterocyclic peptide nanotube. J Am Chem Soc 2003;125(31):9372–6.
[51] Usta M, Wortelboer HM, Vervoort J, Boersma MG, Rietjens IM, van Bladeren PJ, et al. Human glutathione S-transferase-mediated glutathione conjugation of curcumin and efflux of these conjugates in Caco-2 cells. Chem Res Toxicol 2007;20(12):1895–902.
[52] Kokkona M, Kallinteri P, Fatouros D, Antimisiaris SG. Stability of SUV liposomes in the presence of cholate salts and pancreatic lipases: effect of lipid composition. Eur J Pharm Sci 2000;9(3):245–52.
[53] Sohma Y, Sasaki M, Hayashi Y, Kimura T, Kiso Y. Design and synthesis of a novel water-soluble Abeta 1-42 isopeptide: an efficient strategy for the preparation of Alzheimer's disease-related peptide, Abeta 1-42, via O–N intramolecular acyl migration reaction. Tetrahedron Lett 2004;45(31):5965–8.
[54] Taniguchi A, Sohma Y, Hirayama Y, Mukai H, Kimura T, Hayashi Y, et al. "Click peptide": pH-triggered in situ production and aggregation of monomer abeta1-42. Chembiochem 2009;10(4):710–5.
[55] Balducci C, Beeg M, Stravalaci M, Bastone A, Sclip A, Biasini E, et al. Synthetic amyloid-beta oligomers impair long-term memory independently of cellular prion protein. Proc Natl Acad Sci U S A 2010;107(5):2295–300.
[56] Dahlgren KN, Manelli AM, Stine Jr WB, Baker LK, Krafft GA, LaDu MJ. Oligomeric and fibrillar species of amyloid-beta peptides differentially affect neuronal viability. J Biol Chem 2002;277(35):32046–53.

[57] Bravman T, Bronner V, Lavie K, Notcovich A, Papalia GA, Myszka DG. Exploring "one-shot" kinetics and small molecule analysis using the ProteOn XPR36 array biosensor. Anal Biochem 2006;358(2):281–8.
[58] Gobbi M, Re F, Canovi M, Beeg M, Gregori M, Sesana S, et al. Lipid-based nanoparticles with high binding affinity for amyloid-beta(1–42) peptide. Biomaterials 2010;31(25):6519–29.
[59] Lallana E, Fernandez-Megia E, Riguera R. Surpassing the use of copper in the click functionalization of polymeric nanostructures: a strain-promoted approach. J Am Chem Soc 2009;131(16):5748–50.
[60] Yanagisawa D, Shirai N, Amatsubo T, Taguchi H, Hirao K, Urushitani M, et al. Relationship between the tautomeric structures of curcumin derivatives and their abeta-binding activities in the context of therapies for Alzheimer's disease. Biomaterials 2010;31(14):4179–85.